ISSN 1330-3651 (Print), ISSN 1848-6339 (Online)
https://doi.org/10.17559/TV-20230808000859
Original scientific paper

# Enhanced Image Denoising with Diffusion Probability and Dictionary Learning Adaptation

JiLan HUANG*, ZhiXiong JIN

**Abstract:** Image denoising is essential for numerous image processing applications, where image noise can profoundly impact processing efficiency and output quality. Addressing the challenge of inflexible reference images in unconditional diffusion probability models and enhancing image denoising performance is of paramount importance. In this research, we propose a novel image denoising model based on component decoupling and introduce sensitivity decoupling operators to prevent entanglement and redundancy among different decoupling models. Additionally, we leverage a model-driven network to fuse image components, resisting noise and model degradation, thereby aiding network convergence. Subsequently, we construct an image adaptive denoising model incorporating diffusion probability and dictionary learning. Experimental results demonstrate the superiority of the proposed approach over other algorithms in grayscale image processing on the Set12 dataset, achieving a peak signal-to-noise ratio (PSNR) of 35.75 dB and an average structural similarity (SSIM) value of 92.68%. Similarly, on the BSD68 dataset, our algorithm outperforms others with a PSNR of 34.35 dB and an average SSIM of 93.89%. Furthermore, for colour image processing, our method yields higher PSNR and average SSIM compared to other approaches. The findings indicate a significant improvement in denoising effectiveness compared to prior methods, highlighting the practical value of the proposed image denoising algorithm.

**Keywords:** decoupling; denoising; dictionary learning; diffusion probability; image

## 1 INTRODUCTION

The advancement of image processing technology has led to its widespread application across various fields. However, images often suffer from the interference of noise, which hampers efficient information transmission. Therefore, before undertaking any image processing tasks, it is essential to denoise the images to attenuate or eliminate irrelevant information [1]. Image denoising (ID) aims to preserve the main features of the original image while separating the image signal from the noise signal [2]. However, noise in images exhibits diverse distribution characteristics and can be influenced by factors such as image acquisition and transmission, leading to two primary categories: additive noise and quantization noise [3]. Current image denoising methods fall into three main categories: traditional filter-based methods, model-based methods, and deep learning (DL) methods [4].

Convolutional Neural Networks (CNN) have shown outstanding denoising performance, particularly as external prior methods that utilize image constraints to solve the inverse problems they encounter during processing [5]. Through extensive data training and learning, DL-based denoising methods leverage external prior conditions to maximize their effectiveness [6]. Nevertheless, DL technology still possesses certain limitations, resulting in uncontrollable results after processing. To address these limitations, this study adopts the perspective of conditional diffusion and introduces reference images during sampling, incorporating dictionary learning methods for image processing. The addition of sensitivity decoupling operators prevents entanglement and redundancy between different decoupling models. Ultimately, an image adaptive denoising model based on diffusion probability and dictionary learning is constructed, aiming to enhance the efficiency and performance of existing denoising methods while overcoming the drawbacks of conventional convolutional dictionary learning deep unfolding methods.

This research is divided into five key sections. The first section introduces the current status, challenges, and significance of ID. The second section conducts an analysis of domestic and international research outcomes on ID methods, exploring the difficulties and solutions encountered by existing approaches. The third section presents the specific method of ID studied, which is divided into two main components: the design of a deep conditional ID diffusion model and the construction of an image adaptive denoising model (DM) based on diffusion probability and dictionary learning (DIL). In the fourth section, the research method is validated by comparing it with various ID methods on different datasets to evaluate its denoising efficacy. The final section summarizes the research work, highlights future research directions and potential improvements, facilitating future work in this area.

## 2 RELATED WORK

ID is a prerequisite for many other image tasks. By denoising the image and removing any interfering information, it can greatly improve the efficiency of subsequent image processing work. Therefore, ID methods have always been of great concern. Zhang D and other scholars proposed a method that combines Convolutional Neural Networks (CNN) with 3D filtering and block matching to solve the problem of sudden ID. Experiments have shown that this method outperforms other methods for denoising burst images [7]. Wang J. et al. proposed a filtering algorithm combining ID and mathematical morphology to solve the problem that the edge information of the image is blurred in the process of noise removal. The outcomes showcase that this method can markedly improve the edge clarity of ID [8]. Wang Y. and other researchers proposed to use variable exponential fractional reciprocal, integer reciprocal, and book writing regularization methods to achieve ID while preserving the texture details of the image. Research has shown that this method has strong robustness to noise [9]. Usui K. and other researchers used the denoising convolutional neural network (DnCNN) of convolutional neural network as a general CNN model and used it for transfer learning to denoise images. The outcomes showcase that this method has a more significant denoising effect than other ID

methods [10]. Thakur R. S. et al. conducted a comprehensive study on ID methods based on CNN. Research has depicted that FFDNet can effectively achieve spatially varying Gaussian noise [11].

Tian C. and other researchers proposed a Batch Re normalized Denoising Network (BRDNet) ID method to address the difficulty of training convolutional neural networks for denoising tasks. Numerous experiments have shown that this method outperforms most advanced ID methods [12]. Zheng H. and other researchers presented a new deep convolutional dictionary learning (DCDicL) framework for ID. This framework adaptively adjusts the dictionary based on image content by learning prior knowledge of representation coefficients and dictionaries. Research has shown that this method has superior ID performance [13]. Wang Y. and other scholars proposed a blind ID method in view of asymmetric generative adversarial networks. The outcomes showcase that this method has good denoising effect and robustness [14]. Shi K. et al. presented an ID method in view of local and nonlocal regularization fourth-order evolution equations. Experiments have shown that this method demonstrates the superiority of local and non local ID methods [15]. Xu H. et al. presented a denoising method for hyperspectral images in view of structural matrix restoration. Research has shown that this method outperforms most ID methods in visual and quantitative indicators [16].

In summary, current methods in view of DL can effectively solve the problem of Gaussian noise, but there are still some problems. Firstly, the current DL does not have a significant denoising effect on truly noisy images. Secondly, DL models cannot use one model to solve blind Gaussian noise. In addition, as the depth of the network increases, it will hinder ID, and the error of the training model will also increase. Therefore, by extracting DL methods, an innovative image adaptive denoising algorithm in view of diffusion probability and DIL was presented for enhancing the efficiency of ID.

## 3 RESEARCH METHODOLOGY

The entanglement of images and noise can disrupt the transmission of information and affect its quality and details [17]. The goal of ID is for maintaining the main features of the original image as much as possible, which is also a prerequisite for image processing work. Noise has uncertain factors, so it can be understood as a random error identified by probability statistical methods. It is described by the probability distribution of stochastic process. In addition, due to the widespread application of deep neural networks in various fields, research has integrated traditional image modelling techniques such as DIL and sparse coding into deep neural networks for image restoration. Finally, it constructed an image adaptive DM in view of diffusion probability and DIL, and verified its effectiveness.

### 3.1 The Basic Model

Images are often disturbed by noise during their formation and transmission, which affects the information transmission of the image. Therefore, when performing advanced image processing work, it is necessary to perform noise reduction processing on it. ID refers to the suppression, attenuation, and removal of unwanted information that exists in an image, thereby enhancing the effective information of the image and making it easier for the target or object to be distinguished and explained. According to different influencing factors, noise can be separated into additive noise, multiplicative noise, and quantized noise. When the noise is unrelated to the original shape, it is additive noise, and its calculation expression is shown in Eq. (1).

$$f(x,y)=g(x,y)+n(x,y) \tag{1}$$

In Eq. (1), $f(x,y)$ represents the image contaminated by noise; $n(x,y)$ serves as noise; $g(x,y)$ represents a clean image. Whether there is a signal or not, $n(x,y)$ will exist. When the noise is related to the original image, it is called multiplicative noise. It is a virtual product of the original signal and cannot exist independently. During the process of image conversion from analog to digital, there will be certain errors, which are called quantization noise [18]. The purpose of noise reduction is to obtain clean images that are not contaminated by noise from directly visible images. Therefore, the noise reduction model can be depicted by Eq. (2).

$$y=x+n \tag{2}$$

In Eq. (2), $y$ refers to the image that has been contaminated; $n$ represents noise; $x$ represents a clean image. According to the different probability distributions of noise in the image, noise can be divided into 6 types. Among them, the probability density function of Gaussian noise conforms to normal distribution, and its position in the image is random. And since Gaussian noise is the most common, research focuses on it as the focus of image noise removal. Currently, discriminative learning in view of DL can effectively address the Gaussian noise. In DL, deep neural networks (DNNs) have strong representativeness [19]. DNN is composed of convolutional layer, activation layer, pooling layer, and other relevant layer. In image processing, convolution mainly targets a set of multidimensional matrices. At this point, convolution actually involves multiplying the elements that are aggregated into different parts and positions of the convolution kernel matrix, and then summing them up. As shown in Fig. 1, it is the process of convolution operation [20].

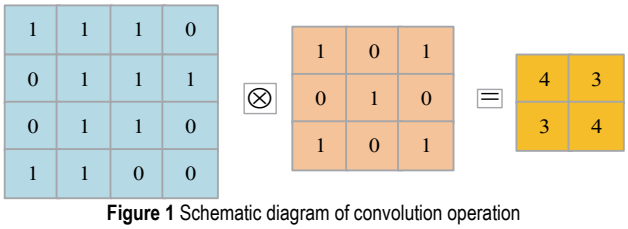


**Figure 1** Schematic diagram of convolution operation

In Fig. 1, the size of the convolutional filter is 3 × 3; The size of the convolutional image matrix is 4 × 4; The step size of convolution is 1. Therefore, the final output result is a feature matrix with a size of 2 × 2. When the step

size of the convolutional filter is set to 1, it represents that the distance each time the convolutional filter moves is 1 unit, which is used for the operation. For image matrices that require convolution, the convolution filter starts from the upper left corner and moves in steps. The loss function can measure the disparity in the predicted value $f(x)$ and the true value $Y$. The lower the loss value, the better the robustness. Meanwhile, it is an important component of the empirical risk function. As shown in Eq. (3), it is the composition of the structural risk function, namely the empirical risk term and the regularization term.

$$\theta^* = \arg\min_{\theta} \frac{1}{N}\sum_{i=1}^{N} L\left(y_i, f\left(x_i,\theta\right)+\lambda\phi\left(\theta\right)\right) \tag{3}$$

In eq. (3), $L$ is the loss function; $\phi(\theta)$ serves as the regular term or penalty term; $\lambda$ serves as measuring the experience line and model complexity. The denoising diffusion probability model is the best generative model in unconditional image generation. It learns Markov chains and gradually transforms simple distributions into data distributions [20]. When potential variables of the same dimension are sequentially used, noise will gradually be added to the data. As shown in Fig. 2, a depth model based on conditional diffusion is designed to drive neural networks to denoise images.

As shown in Fig. 2, assuming the input reference image is $Y$, given a clean data $y_0$, the sampling closed form calculation for noisy image $y_t$ is shown in Eq. (4).

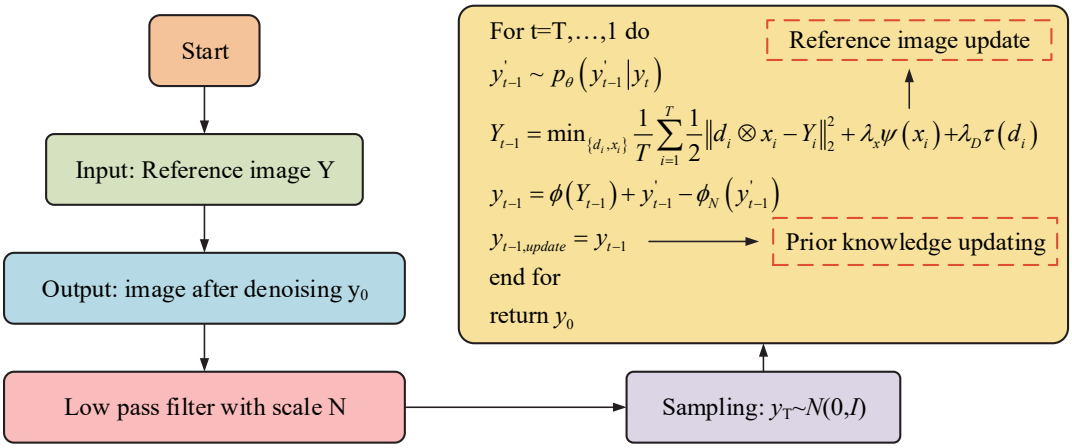


**Figure 2** Image denoising process driven by depth model based on conditional diffusion

$$q\left(y_t|y_0\right) = N\left(y_t;\sqrt{\overline{a_t}}y_0,\left(1-\overline{a_t}\right)I\right) \tag{4}$$

In Eq. (4), $\beta_t$ represents one variance plan; $N$ represents noise; $a_t$–represents the difference between 1 and the variance plan. A method for controlling the unconditional diffusion probability models (DDPM) has been proposed to perform image restoration from a given reference image at each step. Sampling images from the conditional distribution probability of condition $D$, then condition $D$ constrains the transformation $p_\theta\left(y_{t-1}|y_t\right)$. To maintain the dimensionality of the image and make $\varphi_N(\bullet)$ a linear low-pass filtering operation, the Markov variation is shown in Eq. (5).

$$p_\theta\left(y_{t-1}|y_t,D\right) \approx p_\theta\left(y_{t-1}|y_t,\varphi_N\left(y_{t-1}\right)=\varphi_N\left(H_{t-1}\right)\right) \tag{5}$$

In Eq. (5), $H$ represents the result of DIL denoising. The condition $D$ in each transition from $y$ to $y_{t-1}$ can be replaced by a local condition. Among them, the latent variable $y_{t-1}$ shares low-frequency content with the updated reference image $Y$. In each transformation process, the reverse diffusion process is first used to predict $y'_{t-1}$, and then based on each reference image, a low-pass filter is used to maintain the same dimension between the two images. Finally, matching is performed to obtain the denoised image. The calculation expression equation is shown in Eq. (6).

$$\begin{cases} y' \sim p_\theta\left(y'_{t-1}|y_t\right) \\ y_{t-1} = \varphi\left(Y_{t-1}\right)+\left(I-\varphi\right)\left(y'_{t-1}\right) \end{cases} \tag{6}$$

For reference image $Y$, the study adopts a combination of deep convolutional DIL to update, and its calculation expression is shown in Eq. (7)

$$\min_{\{d_i,x_i\}} \frac{1}{T}\sum_{i=1}^{T}\frac{1}{2}\|d_i \otimes x_i - Y_i\|_2^2 + \lambda_x\psi\left(x_i\right)+\lambda_D\tau\left(d_i\right) \tag{7}$$

In Eq. (7), $T$ represents the stage of denoising, corresponding to $t$ in the model. $\tau(d_i)$ and $\psi(x_i)$ represents the dictionary and prior knowledge of the image, respectively.

### 3.2 The Image Adaptive Denoising Model

Although current deep unfolding methods have improved the interpretability of deep unfolding, their performance still lags behind methods based on deep unfolding [21]. Image signals possess an essential influence on traditional image processing applications, and the reconstruction ability of signals can be reconstructed through a good dictionary. Therefore, sparse representation is a key aspect of DIL. A popular method is to linearly combine the atomic bases of image block vectors. As shown in Fig. 3, it is a schematic diagram of dictionary and sparse encoding operations [22].

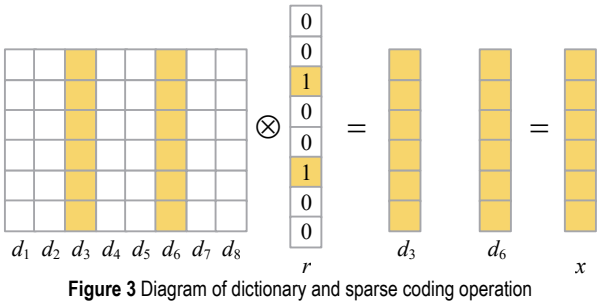


**Figure 3** Diagram of dictionary and sparse coding operation

As shown in Fig. 3, it assumes that the image block vector is $y \in R^m$, and the purpose of DIL is to decompose the dictionary matrix $D$ and sparse code matrix $X$ from the original sample $Y$. Due to the relatively small amount of sparse code $X$ data, it appears sparse. The feature of the original sample $Y$ is stored in dictionary $D$, and its calculation expression is shown in Eq. (8)

$$Y_{m*n} = D_{m*s} * X_{s*n} \tag{8}$$

In Eq. (8), when $s$ is much smaller than $m$ and $n$, the dimensions of $D$ and $X$ will be much lower than the original $Y$. When matrix $X_{s*n}$ is regarded as column vector form $(x_1, x_2, \ldots, x_n)$, Eq. (9) is obtained.

$$Y = D*(x_1, x_2, \ldots, x_n) = D*x_1, D*x_2, \ldots, D*x_n \tag{9}$$

In Eq. (9), $D*x_i$ is the $i$ column vector in $Y$. The DIL (DicL) model can be expressed as Eq. (10) [23].

$$\min_{D,X} \frac{1}{2}\|DX - Y\|_2^2 + \lambda_X \psi(X) + \lambda_D \phi(D) \tag{10}$$

In Eq. (10), $\lambda_X$ and $\lambda_D$ represent the regularization parameters of and respectively; $\psi(X)$ is a sparsity prior, and the corresponding DIL model is commonly referred to as the sparse DIL model. Image decomposition is a classic image processing problem that can effectively extract impurity information from images [24].

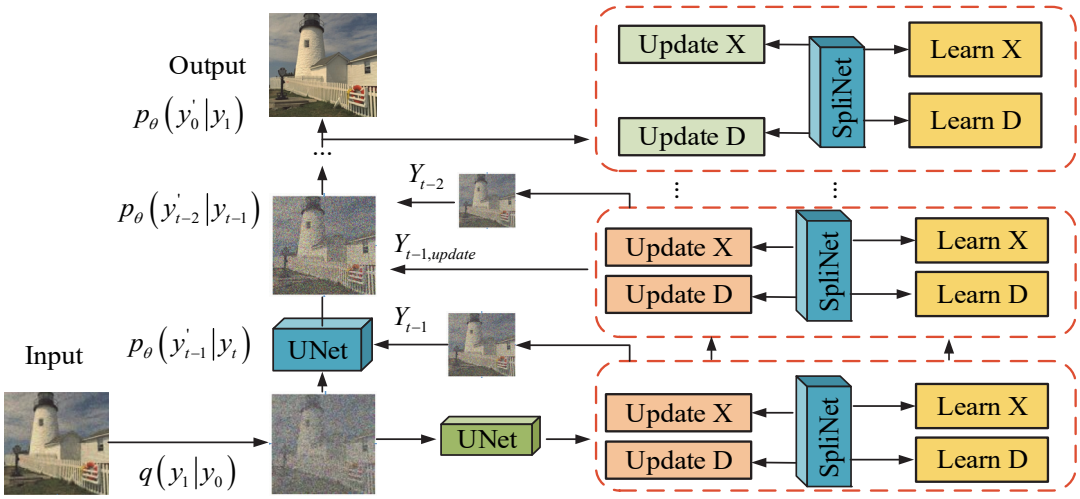


**Figure 4** Image denoising process based on conditional diffusion and dictionary learning model

As shown in Fig. 4, an ID step in view of conditional diffusion and DIL model is designed for the study.

As shown in Fig. 4, in the entire depth conditional diffusion probability model, Gaussian random noise is gradually added to the image through the forward process $q(y_t|y_{t-1})$. The backpropagation neural network architecture follows the backbone of PixelCNN++and is composed of a widened residual network (ResNet) to form a U-Net like structure. In each time stage of reverse diffusion, a deep convolutional dictionary is introduced to learn the denoised image $Y_{t-1}$ from the previous stage as a reference. In deep convolutional DIL, to update the prior of an image, the study uses the denoised image $Y_{t-1,\text{update}}$ of a backpropagation neural network as its updated value. The network architecture of DIL will obtain initial estimates of $X$ for some images through an InputNet network. And it initializes a dictionary $D$, while this article uses UpdateX and LearnX for $X$ update and learning, respectively, for the LearnX network. Each residual unit is composed of two ReLU activated Conv layers and one hop connection. For dictionary $D$ update and learning, this paper uses UpdateD and LearnD respectively. For LearnD network, the research uses a very shallow hop connection structure. Due to the lack of learnable parameters for the forward diffusion process, the $L_T$ in the forward process was used as a constant in training. In the process of reverse diffusion, the study uses the loss function used by PUI SE and StyleGAN, and its definition is shown in Eq. (11).

$$\begin{aligned} L_{\text{total}} &= \left\|\phi(G(z)) - \phi(Y)\right\|_2^2 \\ &+ GEOCROSS(v_1, \ldots, v_{14}) \\ &+ aL_{\text{noise}} \end{aligned} \tag{11}$$

In Eq. (11), the three terms on the right side of the equation are respectively mean square error, geodesic cross loss, and noise regularization. $G(z)$ represents the generated image; $L_{\text{noise}}$ represents noise regularization. The study selected L1 Loss as the loss function for each level of output in DIL, and set the loss weight of the final stage to 1, and the weight of the other stages to $1/T - 1$. To address the limitations of existing deep unfolding methods for convolutional DIL [25], a DM for images based on decoupled deep DIL is proposed. The overall architecture is shown in Fig. 5.

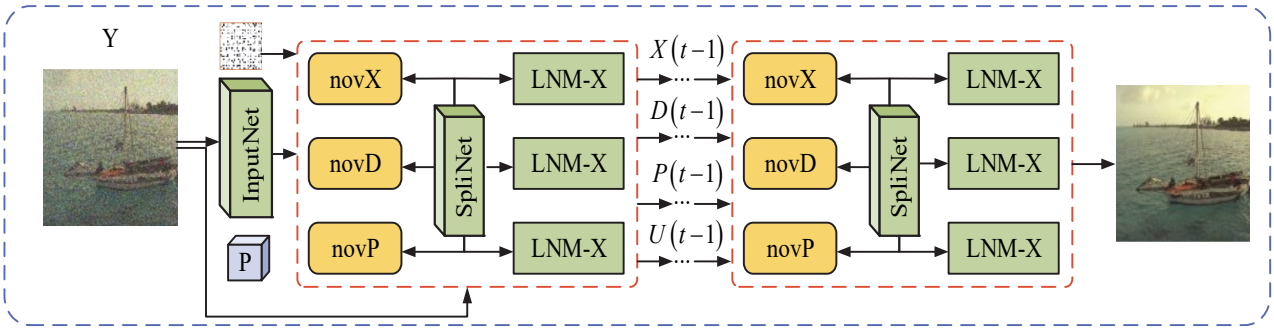


**Figure 5** Image denoising model based on decoupling depth dictionary learning

As shown in Fig. 5, the study constructs an image DM based on component decoupling, and constructs convolutional sparse perception separately. Each part of the image is denoised using an adaptive dictionary. Based on the decoupling model, sensitivity decoupling operator $P$ is added to prevent entanglement and redundancy between different decoupling models. Then it utilizes a model driven network to fuse different components of the image [24]. And it uses this to resist noise and model degradation, help the network converge, and ultimately form a neural network image DM that decouples deep DIL. Eq. (12) represents the expression of the learning model constructed for research.

$$\begin{cases} \min\limits_{\{D_{1,i},X_{1,i},P_{1,i},P_{2,i},X_{2,i}\}} \dfrac{1}{N}\sum\limits_{i=1}^{N}\dfrac{1}{2}\left\|Y-P_{1,i}D_{1,i}\otimes X_{1,i}-P_{2,i}D_{2,i}\otimes X_{2,i}\right\|_2^2+C+M \\ C=\lambda_{X_1}\phi\left(X_{1,i}\right)+\lambda_{X_2}\phi\left(X_{2,i}\right)+\lambda_{D_1}\psi\left(D_{1i}\right) \\ M=\lambda_{D_2}\phi\left(D_{2,i}\right)+\lambda_{P_2}\psi\left(P_{1,i}\right)+\lambda_{P_2}\psi\left(P_{2,i}\right) \end{cases} \tag{12}$$

In Eq. (12), $N$ represents the use of a set of $N$ training sample pairs, with subscripts 1 and 2 representing the basics and details of the image, respectively. To prevent entanglement between different components, this paper introduces the sensitivity decoupling operator $P$ The study evaluated the quality of ID using methods such as Peak Signal to Noise Ratio ($PSNR$) and structural similarity. The quality evaluation of $PSNR$ is in view of the differences in pixels and is also in view of error sensitive image quality evaluation standards. Its calculation expression is shown in Eq. (13) [26].

$$PSNR=10\log_{10}\left(\frac{\left(2^k-1\right)}{MSE}\right) \tag{13}$$

In Eq. (13), $k$ serves as the number of pixel bits, usually taken as 8, representing a pixel gray scale of 256. The higher the value of $PSNR$, the smaller the image distortion. Structural Similarity (SSIM) measures the similarity of images from three: brightness, contrast, and structure. Its calculation expression is shown in Eq. (14).

$$\begin{cases} l\left(X,Y\right)=\dfrac{2\mu_X\mu_Y+C_1}{\mu_X^2+\mu_Y^2+C_1} \\ c\left(X,Y\right)=\dfrac{2\sigma_X\sigma_Y+C_2}{\sigma_X^2+\sigma_Y^2+C_2} \\ s\left(X,Y\right)=\dfrac{\sigma_{XY}+C_2}{\sigma_X\sigma_Y+C_2} \end{cases} \tag{14}$$

In Eq. (14), $l$, $c$, $s$ represents brightness, contrast, and structure, respectively. $\mu_X$, $\mu_Y$ serves as the mean of images $X$ and $Y$. $\sigma_X$, $\sigma_Y$ serves as the variance between image $X$ and $Y$; $\sigma_{XY}$ serves as the covariance of two images; $C_1$, $C_2$, $C_3$ represents constants. To avoid having a denominator of 0, Eq. (15) is derived.

$$\begin{cases} C_1=\left(K_1*L\right)^2 \\ C_2=\left(K_2*L\right)^2 \\ C_3=\dfrac{C_2}{2} \end{cases} \tag{15}$$

In Eq. (15), generally $C_1$, = 0.01, $K_2$ = 0.03 $L$ = 255. In practice, the image can be divided into $N$ blocks by sliding the window. Calculate the structural similarity based on the corresponding blocks of each block, and then add up the structural similarity of all image widths to obtain the average value, which is the average mechanism similarity. Its calculation expression is shown in Eq. (16).

$$MSSIM\left(X,Y\right)=\frac{1}{N}\sum_{K=1}^{N}l\left(X,Y\right)\bullet c\left(X,Y\right)\bullet s\left(X,Y\right) \tag{16}$$

In Eq. (16), the larger the $MSSIM$ value, the smaller the image distortion.

## 4 EXPERIMENTAL RESULTS AND DISCUSSION

The experiment is based on Facebook's open-source Python DL platform, using GPU for all experiments. This

study used the Adam optimizer for parameter updates, setting the size of the Bitch size to 32. And it sets the learning rate of the reverse diffusion process and the learning rate of DIL to 2e-4 and 1e-4, respectively. The learning rate of the DIL module decays by 0.5 times every period of time. To verify the ID performance of depth model driven neural networks based on conditional diffusion, comparative experiments were conducted on four datasets: CBSD68, Kodak24, McMaster, and Urban100. And it compares different denoising methods and research methods on the same dataset. The comparison of ID methods on the CBSD68 dataset are shown in Fig. 6.

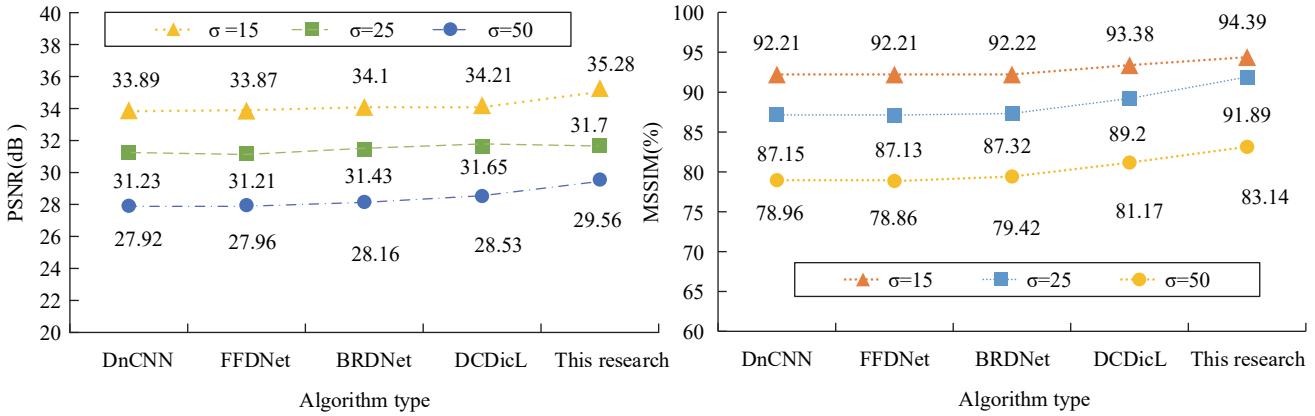


(a) Comparison results of image denoising methods PSNR on dataset CBSD68

(b) Comparison results of image denoising methods MSSIM on dataset CBSD68

**Figure 6** CBSD68 data set comparison results of image denoising methods

Fig. 6a shows that in the CBSD68 dataset, as $\sigma$ increases, the PSNR values obtained by various ID methods all decrease. When $\sigma$ is the same, the PSNR value of the ID algorithm based on research design is higher than other algorithms. When $\sigma$ = 15, the PSNR value of ID based on the research method is the highest, at 35.28 dB. Fig. 6b shows that as $\sigma$ increases, the MSSIM values of each algorithm decrease. When $\sigma$ is the same, the MSSIM value based on the research algorithm is higher than other algorithms. When $\sigma$ = 15, the MSSIM value of ID in view of the research method is the highest, at 94.39%. In summary, the conditional diffusion probability DM studied has the best denoising effect among the five algorithms. As shown in Fig. 7, the comparison of ID methods on the Kodak24 dataset are presented.

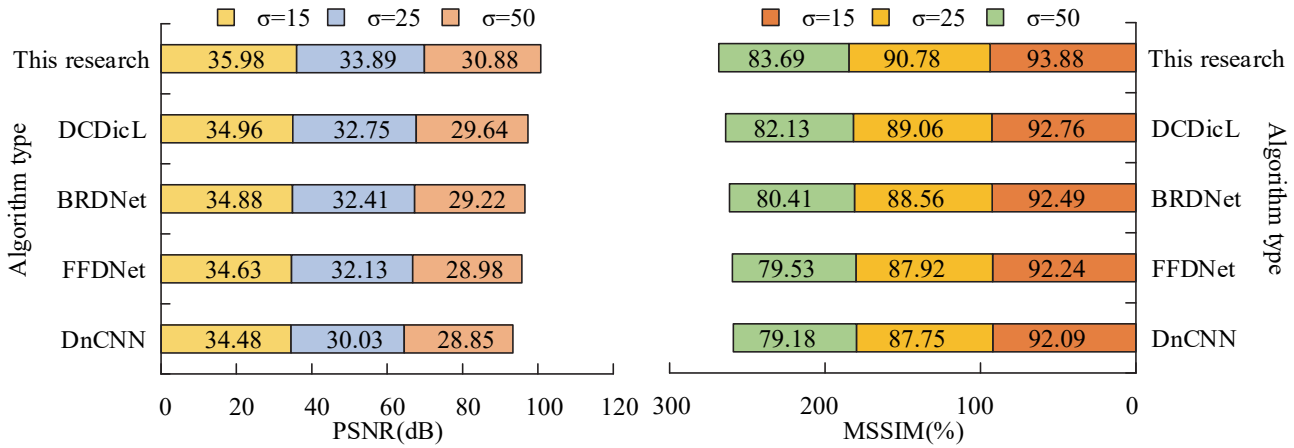


(a) Comparison results of image denoising methods PSNR on dataset Kodak24

(b) Comparison results of image denoising methods MSSIM on dataset Kodak24

**Figure 7** Kodak24 data set comparison results of image denoising methods

Fig. 7a shows that in the Kodak24 dataset, when $\sigma$ is the same, the PSNR value of the ID algorithm based on the research design is higher than that of other algorithms. When $\sigma$ = 15, the PSNR value of ID based on the research method is the highest, at 35.98 dB. Fig. 7b shows that when $\sigma$ is the same, the MSSIM value based on the research algorithm is higher than other algorithms. When $\sigma$ = 15, the MSSIM value of ID based on the research method is the highest, at 93.88%. In summary, it indicates that the research model has the best denoising effect in the Kodak24 dataset. As shown in Fig. 8, the comparison of ID methods on the McMaster dataset are presented.

Fig. 8a shows that in the McMaster dataset, when $\sigma$ = 15, the PSNR value of ID based on the research method is the highest, at 36.49 dB. The MSSIM value of ID based on research methods is the highest, at 94.13%. Figs. 8b and c indicate that the PSNR and MSSIM values of ID based on the research method are higher than all other algorithms. In summary, it illustrates that the research model possesses the optimal denoising outcome in the McMaster dataset.

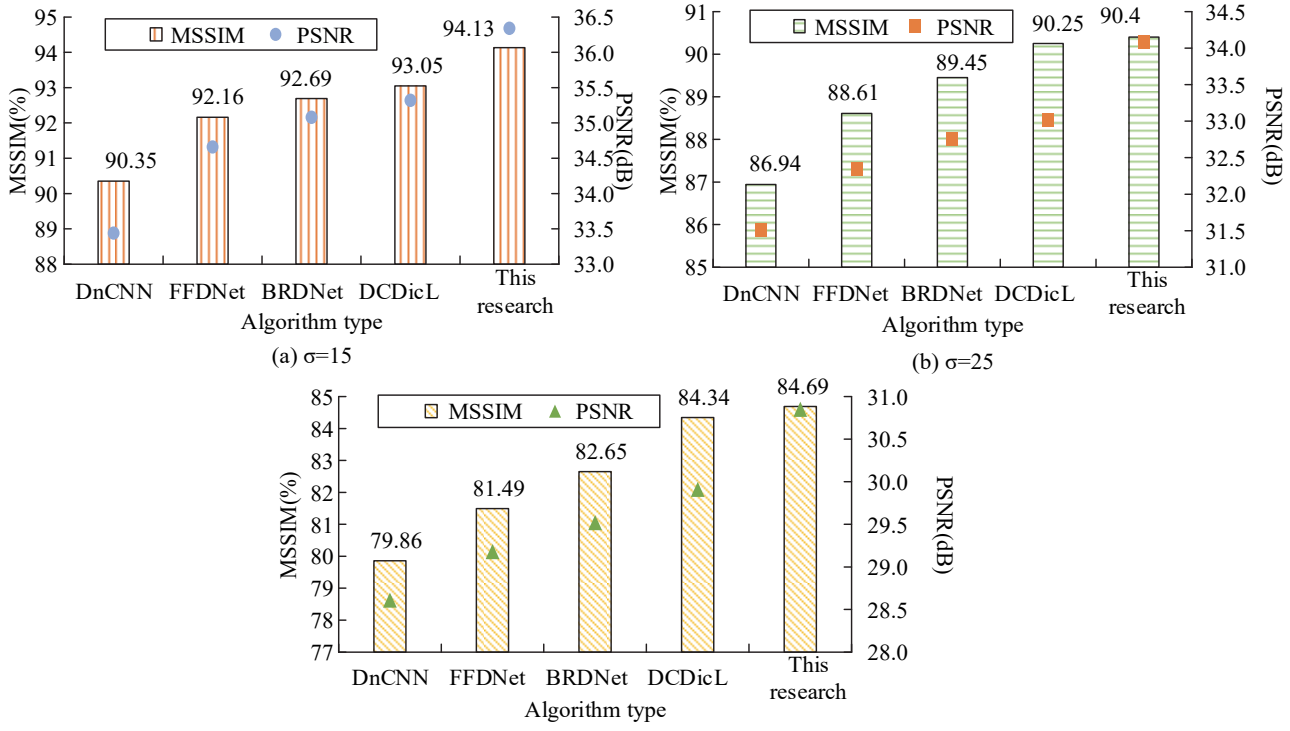


(a) σ=15 (b) σ=25

(c) σ=50

**Figure 8** McMaster data set comparison results of image denoising methods

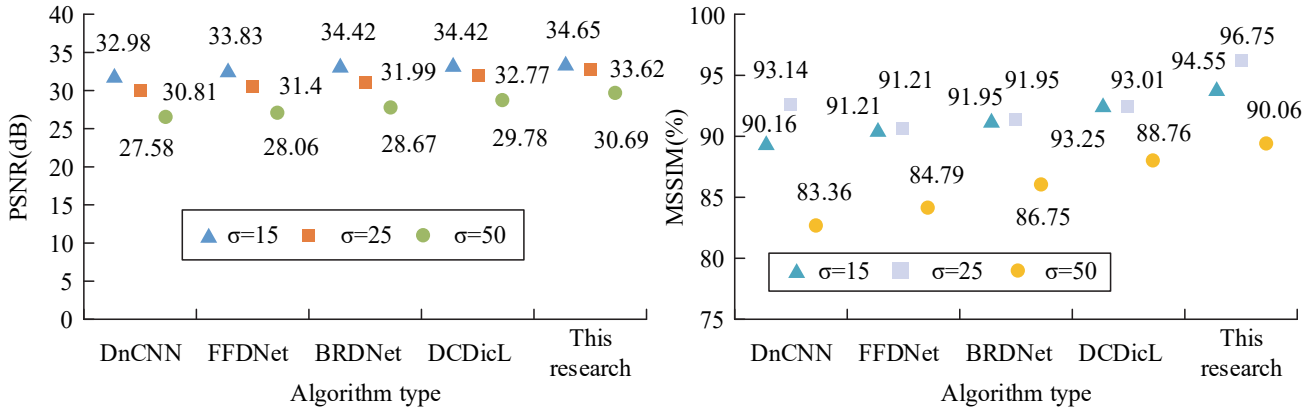


(a) Comparison results of image denoising methods PSNR on dataset Urban100

(b) Comparison results of image denoising methods MSSIM on dataset Urban100

**Figure 9** Urban100 data set comparison results of image denoising methods

As shown in Fig. 9, the outcomes of ID methods on the Urban100 dataset are presented.

Fig. 9a shows that in the Urban100 dataset, when the noise $\sigma$ is the same, the PSNR value of the ID algorithm based on the research design is higher than that of other algorithms. When $\sigma$ = 15, the PSNR value of ID based on the research method is the highest, at 34.65 dB. Fig. 9b shows that when $\sigma$ is the same, the MSSIM value based on the research algorithm is higher than other algorithms. When $\sigma$ = 15, the MSSIM value of ID based on the research method is the highest, at 96.75%. In summary, the research model possesses the optimal denoising outcome in the Urban100 dataset. For comparing the effectiveness of decoupling deep DIL ID with the latest ID methods, the experiment used a combination of BSDS and WED natural original images for training colour images. And Train400 was used as the training set for grayscale images. The space size $K$, subspace depth *sub*, and multiple $n$ of sensitivity decoupling operator $P$ were selected and compared in the experiment. As shown in Fig. 10, the results of the ablation experiment are shown.

Fig. 10a shows that the PSNR value grows with the growth of $K$ value, and the growth rate slows down until $K$ = 5 is reached. Therefore, to balance performance and efficiency, in the later experimental setup, the space size of $P$ is taken as 5. Fig. 10b shows that the PSNR value grows with the growth of *sub* value, but the magnitude of image quality improvement decreases when *sub* exceeds 4. Therefore, in the later experiment, the subnet depth will be set to 4. Fig. 10c shows that at $n$ = 0.1, the PSNR value is the highest, at 31 dB. Therefore, to ensure the efficiency of ID, the multiple of $P$ is set to 0.1.

As shown in Fig. 11, the denoising results of grayscale images on datasets Set12 and BSD68 using different methods are shown.

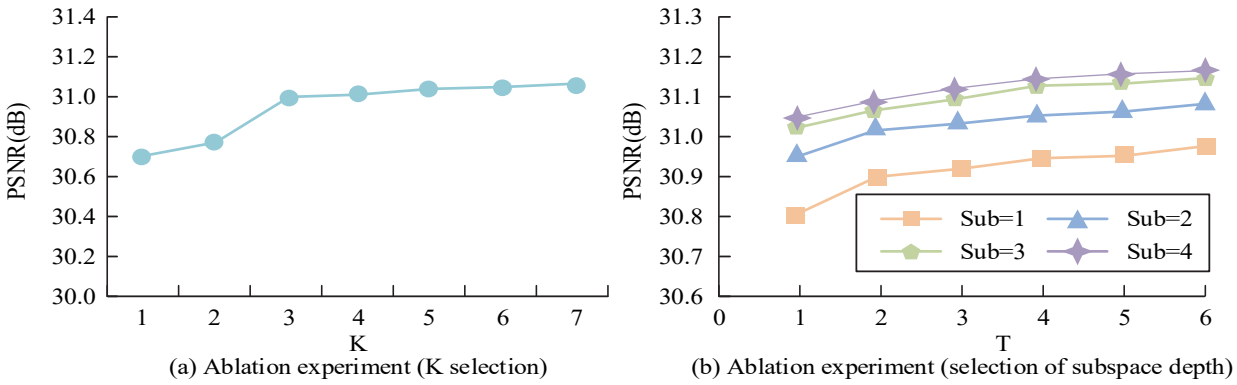


(a) Ablation experiment (K selection)

(b) Ablation experiment (selection of subspace depth)

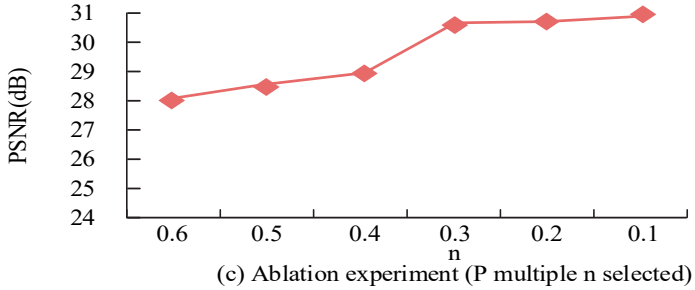


(c) Ablation experiment (P multiple n selected)

**Figure 10** Ablation results

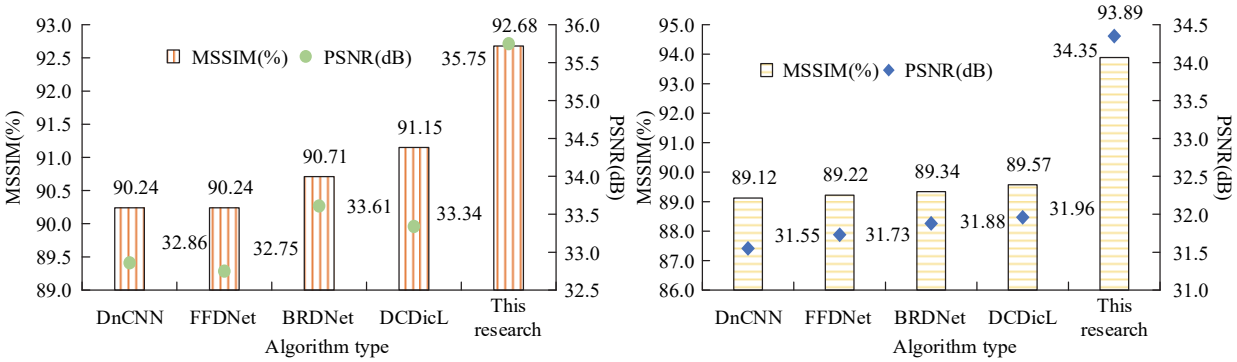


(a) PSNR and MSSIM of gray image denoising results in Set12 data set

(b) PSNR and MSSIM of gray image denoising results in BSD68 data set

**Figure 11** Denoising results of gray image with different methods

Fig. 11a shows that in the Set12 dataset, the PSNR value of the ID algorithm based on the research design is higher than other algorithms, at 35.75 dB. And the MSSIM value of ID based on research methods is also the highest, at 92.68%. Fig. 11b shows that in the BSD68 dataset, the PSNR value of the ID algorithm based on the research design is higher than other algorithms, at 34.35 dB. And the MSSIM value of ID based on research methods is also the highest, at 93.89%. In summary, the decoupling deep DIL grayscale ID method studied has the best denoising effect on the Set12 dataset and the BSD68 dataset. Tab. 1 demonstrates that the comparison of ID effects between different methods on four commonly used colour image datasets.

**Table 1** Comparison of image denoising effects of different methods on four colour image data sets (PSNR (dB)/MSSIM (%))

| Dataset | DnCNN | FFDNet | BRDNet | DCDicL | This research |
|---|---|---|---|---|---|
| CBSD68 | 33.88/92.91 | 33.87/92.91 | 34.10/92.92 | 34.21/92.97 | 35.58/94.65 |
| Kodak24 | 34.48/92.09 | 34.63/92.24 | 34.89/92.48 | 34.97/92.75 | 35.96/94.28 |
| McMaster | 33.45/90.34 | 34.67/92.15 | 35.07/92.68 | 35.31/93.04 | 36.76/93.35 |
| Urban100 | 32.97/93.15 | 33.82/94.18 | 34.48/94.63 | 34.43/94.86 | 35.78/96.73 |

Tab. 1 shows that the denoising method designed in the CBSD68 dataset has the best function. The PSNR and MSSIM values obtained based on the research method are 1.37 dB and 1.68% higher than the performance of second level method DCDicL. In the Kodak24 dataset, the PSNR and MSSIM values based on research methods are 0.99 dB and 1.53% higher than DCDicL. In the McMaster dataset and the Urban100 dataset, the PSNR and MSSIM values based on research methods are still higher than other methods. In summary, it indicates that most of the denoising methods have improved for the colour test set, but the improvement is not as significant as for the grayscale test set. The image adaptive denoising algorithm in view of the diffusion probability and DIL designed in the research has higher PSNR and MSSIM values than other algorithms on various datasets, indicating the effectiveness and superiority of the research method.

## 5 CONCLUSION

In this research, we have addressed the challenge of inflexible reference images in conditional diffusion probability models (DDPM) and aimed to enhance image denoising (ID) performance. We proposed a novel deep unfolding framework that incorporates adaptive dictionary learning (DIL) to dynamically adjust the input image content to the dictionary, ensuring better adaptability. Additionally, the use of decoupling technology effectively mitigates redundancy between noise and images, resulting in improved denoising effects.

Experimental results demonstrate the superiority of the proposed image adaptive denoising algorithm based on research over other ID methods on multiple datasets. The peak signal-to-noise ratio (PSNR) and mean structural similarity (MSSIM) values obtained by our method on the CBSD68, Kodak24, McMaster, and Urban100 datasets surpass those of other algorithms. Specifically, the maximum PSNR values achieved on the four datasets are 35.28 dB, 35.98 dB, 36.49 dB, and 34.65 dB, respectively, while the maximum MSSIM values are 94.39%, 93.88%, 94.13%, and 96.75%, respectively.

For grayscale image processing on the Set12 dataset, our ID algorithm based on research design outperforms other algorithms, achieving a PSNR of 35.75 dB and an MSSIM of 92.68%. Similarly, on the BSD68 dataset, our ID algorithm exhibits better performance with a PSNR of 34.35 dB and an MSSIM of 93.89%. Moreover, for colour image processing, our method consistently achieves higher PSNR and MSSIM values compared to other approaches.

In summary, the image adaptive denoising algorithm based on research demonstrates superior denoising effects on various datasets. While our improved denoising algorithm has shown significant enhancements over other methods, it is worth noting that the improvement for colour testing is not as significant as observed in the grayscale test set. As part of future research, we will focus on addressing this deficiency to further enhance the denoising performance of colour images.

Overall, this study contributes to the field of image denoising by introducing a new approach based on conditional diffusion probability and dictionary learning, showcasing promising results and offering valuable insights for future developments in this area.

## 6 REFERENCES


[1] Ünver, M., Olgun, M., & Türkarslan, E. (2022). Cosine and cotangent similarity measures based on Choquet integral for Spherical fuzzy sets and applications to pattern recognition. *Journal of Computational and Cognitive Engineering*, *1*(1), 21-31. https://doi.org/10.47852/bonviewJCCE2022010105

[2] Choi, D., Kang, S. H., Chan, R. P., & Lee, Y. (2021). Study of the Noise Reduction Algorithm with Median Modified Wiener Filter for T2-weighted Magnetic Resonance Brain Images. *Journal of Magnetics*, *26*(1), 50-59.

[3] Shah, S. H., Wang, X., Abubakar, U., Wang, L., & Gao, P. (2022). Investigation of noise and vibration characteristics of an IPMSM with modular-type winding arrangements having three-phase sub-modules for fault-tolerant applications. *IET Electric Power Applications*, *16*(2), 248-266. https://doi.org/10.1049/elp2.12150

[4] Zheng, M., Zhi, K., Zeng, J., Tian, C., & You, L. (2022). A hybrid CNN for image denoising. *Journal of Artificial Intelligence and Technology*, *2*(3), 93-99. https://doi.org/10.37965/jait.2022.0101

[5] Pan, Y., Ren, C., Wu, X., & Nichols, E. (2022). Real image denoising via guided residual estimation and noise correction. *IEEE Transactions on Circuits and Systems for Video Technology*, *33*(4), 1994-2000. https://doi.org/10.1109/TCSVT.2022.3216681

[6] Singh, A., Pannu, H. S., & Malhi, A. (2022). Explainable Information Retrieval using Deep Learning for Medical images. *Computer Science and Information Systems*, *19*(1), 277-307. https://doi.org/10.2298/csis201030049s

[7] Zhang, D., Zhao, L., Duanqing, X. U., & Dongming, L. U. (2022). Dual-constraint burst image denoising method. *Frontiers in Information and Electronic Engineering: English version*, *23*(2), 220-233. https://doi.org/10.1631/FITEE.2000353

[8] Wang, J., Duan, S., & Zhou, Q. (2021). An Adaptive Weighted Image Denoising Method Based on Morphology. *International Journal of Circuits*, *15*, 271-279. https://doi.org/10.46300/9106.2021.15.31

[9] Wang, Y. & Wang, Z. (2021). Image denoising method based on variable exponential fractional-integer-order total variation and tight frame sparse regularization. *IET Image Processing*, *15*(1), 101-114. https://doi.org/10.1049/ipr2.12010

[10] Usui, K., Ogawa, K., Goto, M., Sakano, Y., Kyougoku, S., & Daida, H. (2021). Quantitative evaluation of deep convolutional neural network-based image denoising for low-dose computed tomography. *Visual computing in Engineering and Medicine*, *4*(1), 199-207. https://doi.org/10.1186/s42492-021-00087-9

[11] Thakur, R. S., Yadav, R. N., & Gupta L. (2019). State-of-art analysis of image denoising methods using convolutional neural networks. *Image Processing*, *IET*, *13*(13), 2367-2380. https://doi.org/10.1049/iet-ipr.2019.0157

[12] Tian, C., Xu, Y., & Zuo, W. (2020). Image denoising using deep CNN with batch renormalization. *Neural Networks*, *121*, 461-473. https://doi.org/10.1016/j.neunet.2019.08.022

[13] Zheng, H., Yong, H., & Zhang L. (2021). Deep convolutional dictionary learning for image denoising. *Proceedings of the IEEE/CVF conference on computer vision and pattern recognition*, *2021*(1), 630-641. https://doi.org/10.1109/CVPR46437.2021.00069

[14] Wang, Y., Chang, D., & Zhao, Y. (2021). A new blind image denoising method based on asymmetric generative adversarial network. *IET Image Processing*, *15*(6), 1260-1272. https://doi.org/10.1049/ipr2.12102

[15] Shi, K. (2023). Coupling local and nonlocal fourth-order evolution equations for image denoising. *Inverse Problems and Imaging*, *17*(3), 686-707. https://doi.org/10.3934/ipi.2022072

[16] Xu, H., Zheng, J., & Qin, M. (2021). Hyperspectral Image Denoising Using Structural Matrix Optimization. *Journal of Computer-Aided Design & Computer Graphics*, *33*(1), 68-80. https://doi.org/10.3724/SP.J.1089.2021.18159

[17] Yang, R. & Li, D. (2022). Adaptive Wavelet Transform Based on Artificial Fish Swarm Optimization and Fuzzy C-means Method for Noisy Image Segmentation. *Computer Science and Information Systems*, *19*(3), 1389-1408. https://doi.org/10.2298/CSIS220321039Y

[18] Salem, S., Saneei, M., & Abbasi-Moghadam, D. (2021). Jitter modeling in digital CDR with quantization noise analysis. *Circuits, Systems, and Signal Processing*, *40*(8), 3884-3906. https://doi.org/10.1007/s00034-021-01653-5

[19] Gomaa, M. M., Mohamed, E. R., Zaki, A. M., & Elnashar, A. (2022). Deep learning to detect image forgery based on image classification. *Journal of System and Management Sciences*, *12*(6), 454-467.

[20] Heiner, M. & Kottas, A. (2022). Estimation and Selection for High-Order Markov Chains with Bayesian Mixture Transition Distribution Models. *Journal of Computational and Graphical Statistics*, *31*(1), 100-112. https://doi.org/10.1080/10618600.2021.1979565
[21] Ghaleb, M. S., Ebied, H. M., Shedeed, H. A., & Tolba, M. F. (2022). Image retrieval based on deep learning. *Journal of System and Management Sciences*, *12*(2), 477-496.
[22] Zhang, H., Lin, J., Hua, J., & Tong, T. (2022). Interpretable convolutional sparse coding method of Lamb waves for damage identification and localization. *Structural Health Monitoring*, *21*(4), 1790-1804. https://doi.org/10.1177/1475921721104
[23] Hajjaj, M. (2022). Joint dictionary and deep learning for cosparse recovery of the millimeter wave massive MIMO channels. *The Journal of Engineering*, *2022*(3), 371-376. https://doi.org/10.1049/tje2.12120
[24] Tan, V. & Loh, Y. P. (2022). Dashboard camera view vehicle license plate compliance verification. *Journal of Logistics, Informatics and Service Science*, *9*(4), 37-50.
[25] Lee, Y. S. (2022). A study on abnormal behavior detection in CCTV images through the supervised learning model of deep learning. *Journal of Logistics, Informatics and Service Science*, *9*(2), 196-209.
[26] Suriyan, K., Ramaingam, N., Rajagopal, S., Sakkarai, J., Asokan, B., & Alagarsamy, M. (2022). Performance analysis of peak signal-to-noise ratio and multipath source routing using different denoising method. *Bulletin of Electrical Engineering and Informatics*, *11*(1), 286-292. https://doi.org/10.11591/eei.v11i1.3332

**Contact information:**
**JiLan HUANG**, Master degree, Associate Professor
(Corresponding author)
Geely University of China,
641423, ChengDu China
E-mail: hlhuanglan@163.com

**ZhiXiong JIN**, Bachelor degree, Associate Professor
Geely University of China,
641423, ChengDu China
E-mail: jinzhixiong@hongyicg.com